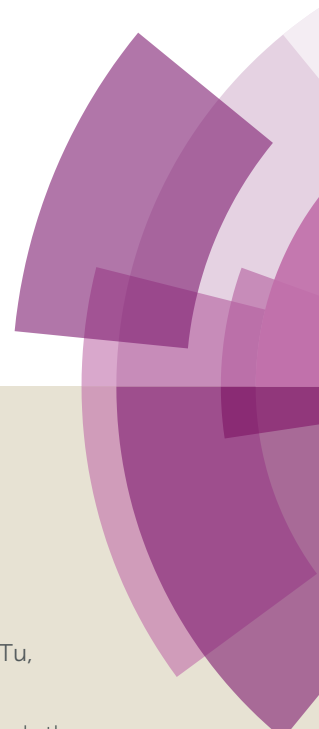


Journal of Materials Chemistry C

Accepted Manuscript



This article can be cited before page numbers have been issued, to do this please use: G. Lu, L. Liu, Z. Tu, Y. Zhou and Y. Zheng, *J. Mater. Chem. C*, 2018, DOI: 10.1039/C8TC06010J.



This is an Accepted Manuscript, which has been through the Royal Society of Chemistry peer review process and has been accepted for publication.

Accepted Manuscripts are published online shortly after acceptance, before technical editing, formatting and proof reading. Using this free service, authors can make their results available to the community, in citable form, before we publish the edited article. We will replace this Accepted Manuscript with the edited and formatted Advance Article as soon as it is available.

You can find more information about Accepted Manuscripts in the [author guidelines](#).

Please note that technical editing may introduce minor changes to the text and/or graphics, which may alter content. The journal's standard [Terms & Conditions](#) and the ethical guidelines, outlined in our [author and reviewer resource centre](#), still apply. In no event shall the Royal Society of Chemistry be held responsible for any errors or omissions in this Accepted Manuscript or any consequences arising from the use of any information it contains.

ARTICLE

Two green iridium(III) complexes containing the electron-transporting group of 4-phenyl-4*H*-1,2,4-triazole for highly efficient OLEDsGuang-Zhao Lu^{1,2,3}, Liang Liu², Zhen-Long Tu², Yong-Hui Zhou^{1*}, You-Xuan Zheng^{2*}Cite this: DOI:
10.1039/x0xx00000xReceived 00th January 2012,
Accepted 00th January 2012

DOI: 10.1039/x0xx00000x

www.rsc.org/

Two new iridium(III) cyclometalated complexes (**Ir-TN₃T** and **Ir-TN₄T**) with 2',6'-bis(trifluoromethyl)-2,3'-bipyridine (TN₃T) and 2',6'-bis(trifluoromethyl)-2,4'-bipyridine (TN₄T) as the cyclometalated ligands and 2-(4,5-diphenyl-4*H*-1,2,4-triazol-3-yl)phenol (dptp) as the ancillary ligand were developed. Both complexes are green phosphors with high photoluminescence quantum efficiency yields ($\lambda_{\text{max}} = 540 \text{ nm}$, $\Phi = 71.2\%$ for **Ir-TN₃T** and $\lambda_{\text{max}} = 513 \text{ nm}$, $\Phi = 91.0\%$ for **Ir-TN₄T**, respectively) in CH₂Cl₂ solutions at room temperature. The organic light emitting diodes (OLEDs) with the single-emitting-layer and double-emitting-layer structures show good performances. Particularly, device **D2** with double-emitting-layer structure based on complex **Ir-TN₄T** with 8 wt% doped concentration shows superior performances with a peak current efficiency of 94.29 cd A⁻¹ and a peak external quantum efficiency (EQE_{max}) of 31.43%, and the efficiency roll-off is mild. When the luminance reaches to 10000 cd m⁻², the EQE value can still be kept at 30.26%. This study demonstrates that the Ir(III) complexes containing ancillary ligand attached with the electron-transporting group 4-phenyl-4*H*-1,2,4-triazole group could facilitate charge trapping across the bulk of the device and have promising application in OLEDs.

Introduction

Interest in cyclometalated iridium(III)¹ and platinum(II)² complexes has soared over the past decade following the demonstration of their potential application in the manufacture of highly efficient light-emitting devices (OLEDs). The spin-orbit coupling exerted by the heavy metal effect allows the harvest of both singlet and triplet electro-generated excitons in devices, leading to a theoretically achievable 100% internal quantum efficiency.³ In the past years, extensive studies of the effect of modifications of the phenylpyridine ligands on the photophysical properties have been carried out.⁴ By introducing electron-withdrawing group CF₃ or more nitrogen atoms into the phenyl rings of ppy, the photophysical and electrochemical properties of Ir(III) or Pt(II) complexes can be tuned. Furthermore, the good electron transport property of these emitters is also important for efficient OLEDs in view of the better hole transport ability of hole transport materials than the electron transport ability of electron transport materials.⁵ Many research groups reported efficient devices based on complexes containing cyclometalated and ancillary ligands with nitrogen, oxygen, phosphorus, sulphur and boron-heterocyclic derivatives for better electron mobility.⁶ For example, some high-performance phosphorescent OLEDs were reported by our group employing Ir(III) emitters with the tetraphenylimidodiphosphinate, oxadiazole and thiadiazole derivatives containing electron-transporting groups as ancillary ligands, which may improve the electron mobility of the Ir(III)

complexes and benefit their OLEDs performances.⁷

Triazole derivatives have received considerable attention in electro/opto-active materials due to their high electron affinity, high photoluminescence quantum yield and good thermal and chemical stability, which make them good candidates for electron injection and transportation materials.⁸ In the last several years, the highly efficient electron-type and bipolar host materials containing the 4-phenyl-4*H*-1,2,4-triazole group as the electron transporting unit have been widely studied.⁹ Additionally, several groups like Huang et. al., Kim et. al. and Chi et. al. have also reported efficient Ir(III) complexes using triazole derivatives as cyclometalated ligands to increase their electron transporting ability and consequently facilitate charge trapping across the bulk for high performance OLEDs.¹⁰ However, few heteroleptic Ir(III) complexes containing the group 4-phenyl-4*H*-1,2,4-triazole as ancillary ligands have been reported, which have more nitrogen heterocycles compared to oxadiazole and thiadiazole, which is beneficial for their device performances. In addition, the two bulky -CF₃ substituents on the phenyl rings of ppy and the three benzene rings spatially distributed on triazole can affect the molecular packing and the steric protection around the metal can suppress the self-quenching behavior.¹¹ From our former study, the Ir(III) complexes with 2',6'-bis(trifluoromethyl)-2,3'-bipyridine (TN₃T) and 2',6'-bis(trifluoromethyl)-2,4'-bipyridine (TN₄T) as the cyclometalated ligands show good electron mobility and high photoluminescence quantum yield (PLQY). On this basis, as is shown in Fig. 1, we designed and synthesized two

new heteroleptic Ir(III) complexes containing TN₃T and TN₄T as the cyclometalated ligands and 2-(4,5-diphenyl-4*H*-1,2,4-triazol-3-yl)phenol (dtp) as the ancillary ligand.¹² Both complexes (**Ir-TN₃T** and **Ir-TN₄T**) show green emission with PLQY up to 91.0%. Using them as emitters, the OLEDs also show good performances with a peak current efficiency of 94.29 cd A⁻¹ and a peak external quantum efficiency of 31.43% with mild efficiency roll-off.

Results and discussion

Preparation and characterization of compounds

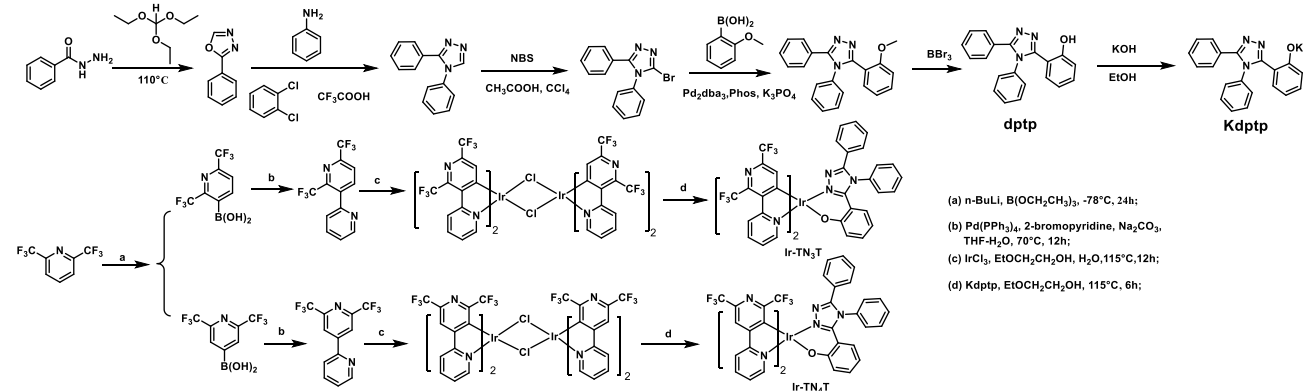


Fig. 1 The synthetic routes of **Ir-TN₄T** and **Ir-TN₃T**.

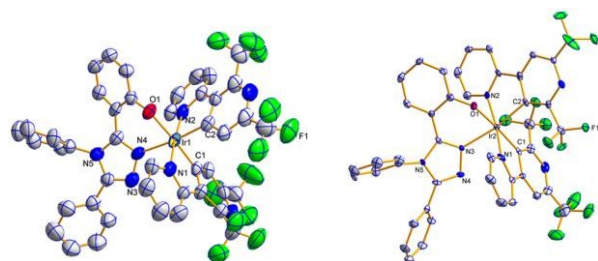


Fig. 2 Oka Ridge Thermal Ellipsoidal plot (ORTEP) diagrams of **Ir-TN₃T** (left, CCDC No. 1832350) and **Ir-TN₄T** (right, CCDC No. 1832348) complexes with the atom-numbering schemes. Hydrogen atoms are omitted for clarity. Ellipsoids are drawn at 50% probability level.

Single crystals of **Ir-TN₃T** and **Ir-TN₄T** were obtained by vacuum sublimation. Fig. 2 shows the Oak Ridge thermal ellipsoidal plot (ORETP) diagrams of the complexes given by X-ray analysis. Selected parameters of the molecular structures and tables of atomic coordinates were collected in the Table S1 and Table S2. As shown in Fig. 2, both complexes have distorted octahedral coordination geometry around iridium center by three chelating ligands with *cis*-C-C and *trans*-N-N dispositions, in which the N-Ir-N angles are all almost around 175.0° and 172.0°, respectively. The Ir-C bond lengths are 1.957-2.032 Å and the Ir-N bonds lengths are 2.017-2.058 Å, respectively, and these values are similar to those reported in other mononuclear Ir(III) complexes.¹³

As shown in Fig. 1, the cyclometalated ligands TN₃T and TN₄T and the ancillary ligand dtp were synthesized according to the reported publications.¹² The Ir(III) complexes were prepared by the reaction of corresponding chloride-bridged dimers [(C[^]N)₂Ir(μ-Cl)]₂ with Kdtp to give the products **Ir-TN₃T** and **Ir-TN₄T**. Purification of the mixture by silica gel chromatography provided crude products, which were further purified by vacuum sublimation. All the new compounds were fully characterized by ¹H NMR spectrometry, high-resolved mass (HR-MS) spectrometry and elemental analysis, and the crystal structures further confirmed the identity of the complexes.

The thermal stability of the emitters is important for the stable OLEDs. In this cases, the thermal properties of the two Ir(III) complexes were characterized by thermogravimetric (TG) measurements under a nitrogen steam. From the TG curves in Fig. S1, it can be observed the decomposition temperatures (5% loss of weight) of TN₃T and **Ir-TN₄T** complexes are as high as 350 °C and 394 °C, respectively. And the good stability of the complexes suggested they are suitable for application in OLEDs.

Electrochemical properties and theoretical calculation

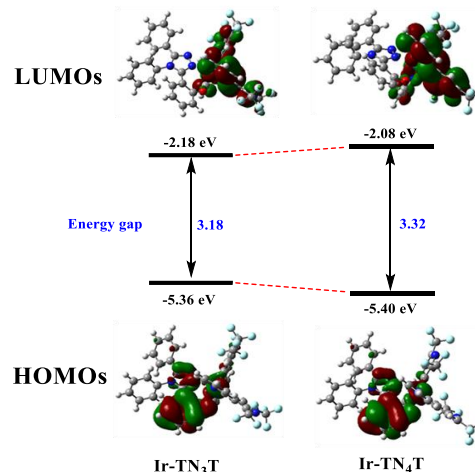


Fig. 3 Molecular orbital diagram for the HOMOs/LUMOs and their energy levels of **Ir-TN₃T** and **Ir-TN₄T** calculated in CH₂Cl₂.

The highest occupied molecular orbital (HOMO) and lowest unoccupied molecular orbital (LUMO) energy levels of the dopants are important for the design of the OLED structure. In order to determine the HOMO/LUMO values of the **Ir-TN₃T** and **Ir-TN₄T**, their electrochemical properties were investigated by cyclic voltammetry in deaerated CH₂Cl₂, relative to an internal ferrocenium/ferrocene reference (Fc⁺/Fc) (Figure S2). The cyclic voltammograms of the complexes in the positive range show strong oxidation peaks, while the reduction peaks are not obvious, demonstrating that the redox process of the complexes is not reversible completely. It is observed that the difference of the HOMO/LUMO values of the iridium complexes is not obvious from the Table 1, in which the LUMOs levels all stay at -2.91 eV and their HOMO levels (-5.34 eV and -5.40 eV) remain almost the same. These values are much higher than those Ir(III) complexes with TNT cyclometalated ligands,¹² suggesting the dtp can increase the HOMO and LUMO energy levels.

To determine the HOMO/LUMO distributions of the Ir(III) molecules and further investigate their electronic structures, the density functional theory (DFT) calculations were performed and the detailed results of the theoretical calculations are included in the SI. As shown in Fig. 3, the HOMO orbitals of two Ir(III) complexes mostly located on the ancillary ligands (77.83% and 77.54%) with a small portion of the cyclometalated ligands (8.20% and 6.94%) and *d*- orbitals of iridium atom (13.97% and 15.52%). The LUMO is mostly distributed over the π* orbitals of the cyclometalated ligands (94.66% and 94.18%) and to a small extent on Ir *d* orbitals (3.45% and 3.02%) and ancillary ligands (1.89% and 2.80%). And the calculated HOMO levels (-5.357 eV and -5.400 eV) fit well with the electrochemical results (-5.340 eV and -5.400 eV) (Table 1).

Photophysical property

The UV-vis absorption spectra of the complexes **Ir-TN₃T** and **Ir-TN₄T** in CH₂Cl₂ at 5 × 10⁻⁵ M are shown in Fig. 4(a), and the

electronic absorption data are listed in Table 1. The absorption spectra of both complexes shows intense bands with extinction below 350 nm, which are assigned to the spin-allowed intraligand (π→π*) transition of cyclometalated ppy derivatives and ancillary ligand. The lower-energy absorption bands in the range 350-500 nm can be assigned to the mixing of ¹MLCT and ³MLCT (metal-to-ligand charge-transfer) transitions, or LLCT (ligand-to-ligand charge-transfer) transition through strong spin-orbit coupling of iridium atom.¹⁴ Compared with complex **Ir-TN₃T** in CH₂Cl₂ with a emission band at 540 nm at RT, complex **Ir-TN₄T** shows blue-shifted emission at 513 nm with much stronger intensity (Fig. 4(b)), which fits well the energy gap calculated by the theoretical calculation and electrochemical analysis. Additionally, the PL quantum yields for **Ir-TN₃T** and **Ir-TN₄T** are 71.2% and 91.0%, respectively. These results suggest that the change of the nitrogen atom position on the phenyl ring affect the emitting properties of Ir(III) complexes greatly. Furthermore, the lifetimes are in the range of microseconds for both complexes (1.47 μs for **Ir-TN₃T** and 1.54 μs for **Ir-TN₄T**, respectively) (Fig. S3). The short lifetimes would improve the spin-state mixing and suppress the excitons annihilation.

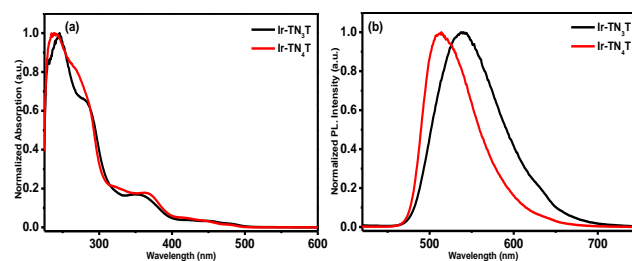


Fig. 4 The UV-vis absorption (a) and emission (b) spectra of complexes **Ir-TN₃T** and **Ir-TN₄T** in degassed dichloromethane (5 × 10⁻⁵ M) at room temperature.

Table 1. Photophysical data of two iridium complexes.

Complex	<i>T_d</i> ^{a)} (°C)	λ_{abs} ^{b)} (nm)	λ_{em} ^{b)} (nm)	Φ ^{c)} (%)	τ ^{b)} (μs)	HOMO/LUMO ^{d)} (eV)	Energy Gap (eV)
Ir-TN₃T	350	244/358	540	71.2	1.47	-5.34/-2.91	2.43
Ir-TN₄T	394	237/369	513	91.0	1.54	-5.40/-2.91	2.49

^{a)} Decomposition temperature; ^{b)} measured in degassed CH₂Cl₂; ^{c)} Φ : emission quantum yields were calculated with *fac*-Ir(ppy)₃ standard in degassed CH₂Cl₂ solution ($\Phi_{\text{P}} = 0.4$); ^{d)} HOMO (eV) = $-(E_{\text{ox}} - E_{1/2, \text{Fc}}) - 4.8$, LUMO (eV) = HOMO + E_{bandgap} .

OLEDs performance

To illustrate the electroluminescent properties of both complexes, typical OLEDs using two complexes as dopants were fabricated. Firstly, the device configuration consists of single emissive layer with ITO / HAT-CN (dipyrazino[2,3-*f*:2',3'-*h*]quinoxaline-2,3,6,7,10,11-hexacarbonitrile, 5 nm) / TAPC (di-[4-(*N,N*-ditolylamino)phenyl]cyclohexane, 50 nm) /

Ir-TN₃T and **Ir-TN₄T** (x wt%) : 2,6DCzPPy (2,6-bis(3-(carbazol-9-yl)phenyl)pyridine, 16 nm) / TmPyPB (1,3,5-tri[(3-pyridyl)-phen-3-yl]benzene, 50 nm) / LiF (1 nm) / Al (100 nm) are named as **S1** and **S2**, respectively. As shown in Fig. 5, the materials of HAT-CN and LiF served as hole- and electron-injecting interface modified materials, respectively. The bipolar 2,6DCzPPy was chosen as host material. The TAPC with high HOMO level (-5.5 eV) acts as electron-donating and hole-

transport media, while TmPyPB with low LUMO level (-2.7 eV) used as electron-accepting and electron-transport material. The HOMO and LUMO levels of Ir(III) complexes were all embedded between those of 2,6DCzPPy (HOMO = 6.10 eV, LUMO = 2.60 eV). Thus, efficient energy transfer from the host to Ir(III) complexes occurred in the emitting layer (EML). All the devices were optimized and the details of optimizing the doping concentration of Ir(III) emitters are included in the SI. The electroluminescence (EL) spectra, current density (J)-voltage (V)-luminance (L), current efficiency (η_c) and power efficiency (η_p) versus luminance, and EQE as a function of luminance characteristics of the devices are displayed in Fig. 6, and the parameters of these devices are summarized in Table 2.

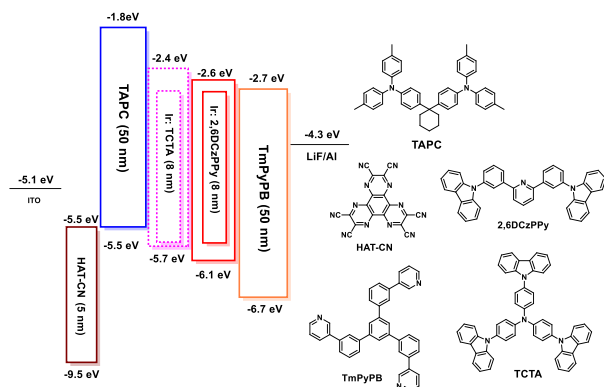


Fig. 5 Energy level diagram of HOMO and LUMO levels (relative to vacuum level) for materials investigated in this work and their molecular structures.

Fig. 6(a) shows the normalized EL spectra of the devices measured at the voltage of 4.0 V with peaks at about 518 nm and 500 nm for devices **S1** and **S2**, which are close to the PL spectra of the Ir(III) complexes in CH_2Cl_2 solutions, indicating that the EL emissions of the devices originate from the triplet excited states of the phosphors in which the CIE coordinates fall in the green region. Due to the same ancillary ligand and similar molecular structures, the device performances of both materials mainly depend on their PL efficiencies and electrochemical properties.

Respectively, the device **S1** (Φ_p of **Ir-TN₃T** is 71.2%) at the 6 wt% concentration shows the maximum luminance (L_{max}) above 40588 cd m^{-2} , the peak current efficiency ($\eta_{c,\text{max}}$) of 83.93

cd A^{-1} and the peak power efficiency ($\eta_{p,\text{max}}$) of 49.76 lm W^{-1} and a maximum external quantum efficiency (EQE_{max}) of 24.25%. Relatively, the device **S2** (Φ_p of **Ir-TN₄T** is 91.0%) at the 8 wt% concentration displays better performances with the L_{max} , $\eta_{c,\text{max}}$ and EQE_{max} of 32085 cd m^{-2} , 88.12 cd A^{-1} and 29.41%, respectively.

In order to further improve the EL performances of these complexes, a hole transport material TCTA (4,4',4'-tris(carbazol-9-yl)triphenylamine) was introduced as another host due to its suitable HOMO level (-5.70 eV) between TAPC and 2,6DCzPPy and the holes and electrons will be distributed in more balanced emissive layers and the exciton recombination zone is expected to be broadened in the double-emitting layer devices. The OLEDs with double emissive layers with the configuration of ITO / HAT-CN (5 nm) / TAPC (50 nm) / Ir(III) complexes (x wt%) : TCTA (8 nm) / Ir complexes (x wt%) : 2,6DCzPPy (8 nm) / TmPyPB (50 nm) / LiF (1 nm) / Al (100 nm) using the dopants of **Ir-TN₃T** and **Ir-TN₄T** are named as **D1** and **D2**, respectively. The corresponding EL characteristics of the devices are shown in Fig. 6, and the detailed results are also summarized in Table 2. Compared to the single-emitting-layer devices, the double-emitting-layer devices exhibit lower turn-on voltages due to the stepwise changed HOMO energy levels of TAPC (-5.5 eV), TCTA (-5.7 eV) and 2,6DCzPPy (-6.1 eV) and the gradual changed LUMO energy levels of TmPyPB (-2.7 eV), 2,6DCzPPy (-2.6 eV) and TCTA (-2.4 eV), which are beneficial for the hole/electron injection and transport. For complex **Ir-TN₃T**, the double-emitting layer device **D1** exhibit slightly inferior performances compared to the single-emitting layer device **S1** with the $\eta_{c,\text{max}}$ and EQE_{max} of 72.77 cd A^{-1} and 20.90%, respectively owing to the imbalance of electron and hole transporting properties of the hole-type host TCTA. However, for complex **Ir-TN₄T** with very high PL efficiency, the double-layer emitting layer device **D2** exhibit better performances than the single-emitting-layer device **S2** with the $\eta_{c,\text{max}}$ and EQE_{max} of 94.29 cd A^{-1} and 31.43%, respectively, which is among the best results of those devices based on Ir(III) complexes.¹⁵ Furthermore, both devices show low efficiency roll-off. When the luminance reached to 10000 cd m^{-2} , the EQE_{max} data of **D1** and **D2** can still be kept at 20.74% and 30.26%, respectively.

Table 2. EL performances of the devices **S1-S2** and **D1-D2**.

Device	$V_{\text{turn-on}}^{\text{a}}$ (V)	L_{max} (cd m^{-2})	$\eta_{c,\text{max}}$ (cd A^{-1})	$\eta_{\text{ext,max}}$ (%)	$\eta_{p,\text{max}}$ (lm W^{-1})	η_c^{b} (cd A^{-1})	$\eta_{\text{ext}}^{\text{b}}$ (%)	CIE (x, y)
S1 (6%)	3.9	40588	83.93	24.25	49.76	82.91	23.94	(0.286, 0.613)
S2 (8%)	3.7	32085	88.12	29.41	49.37	83.69	27.92	(0.203, 0.592)
D1 (6%)	3.6	39888	72.77	20.90	44.82	72.38	20.74	(0.285, 0.612)
D2 (8%)	3.5	39638	94.29	31.43	57.14	90.87	30.26	(0.213, 0.588)

^a) Applied voltage recorded at a luminance of 1 cd m^{-2} ; ^b) Recorded at 10000 cd m^{-2} .

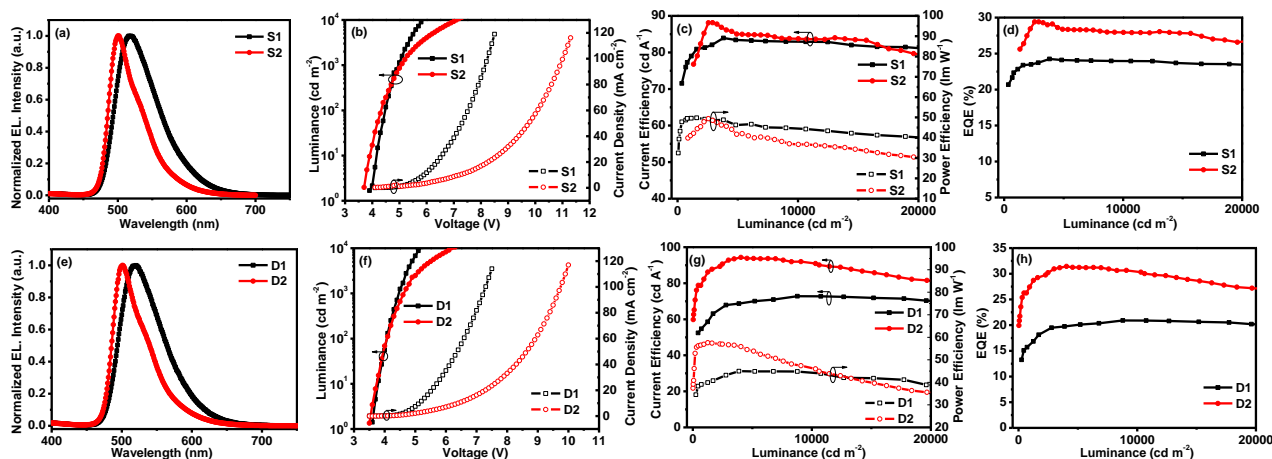


Fig. 6 Characteristics of single-emitting-layer: (a) EL spectra, (b) J - V - L , (c) η_c - L - η_p , (d) EQE - L and characteristics of double-emitting-layer devices: (e) EL spectra, (f) J - V - L , (g) η_c - L - η_p , (h) EQE - L .

The good device performances of the complexes may be due to their possible good electron mobility for the reason that the hole mobility of the TAPC is higher than the electron mobility of the TmPyPB in OLEDs,⁵ the excitons accumulation is expected in hole blocking layer (TmPyPB) near the interface of emitting layer (Ir(III) complexes (x wt%): 2,6DCzPPy) / TmPyPB.¹⁶ The accumulation of excitons is expected to cause the serious triplet-triplet annihilation (TTA) and triplet-polaron annihilation (TPA) of the iridium complexes, and high efficiency roll-off consequently. From our former study we knew both the TN₃T and TN₄T ligands are beneficial for the electron mobility of the Ir(III) complexes, and due to the nitrogen heterocycle structure, the application of **dptp** as the ancillary ligand also has the same effect.

Conclusions

In conclusion, two cyclometalated Ir(III) complexes **Ir-TN₃T** and **Ir-TN₄T** with 2',6'-bis(trifluoromethyl)-2,3'-bipyridine and 2',6'-bis(trifluoromethyl)-2,4'-bipyridine as the cyclometalated ligands and 2-(4,5-diphenyl-4H-1,2,4-triazol-3-yl)phenol as the ancillary ligand were successfully investigated and applied in the OLEDs. The OLEDs based on complexes **Ir-TN₃T** and **Ir-TN₄T** with single and double emissive layers showed high EQE_{max} as 24.25% and 31.43%, respectively and also showed slow roll-off. When the luminance reaches to 10000 $cd\ m^{-2}$, the EQE values can still be kept at 23.94% and 30.26%, respectively. This study suggested that the nitrogen heterocycle cyclometalated ligands and ancillary ligands could be employed well in Ir(III) complexes, which would have potential applications in OLEDs.

Experimental Section

The general information for the sample and device

measurement were listed in the SI. The synthesis of the ligands and complexes were performed under nitrogen atmosphere. All reagents and chemicals were purchased from commercial sources and used without further purification.

2-Phenyl-1,3,4-oxadiazole. Benzhydrazide (21.66 g, 159.0 mmol) and triethyl orthoformate (90 mL) were placed in a 500 mL, two-neck round-bottom flask, and the mixture was vigorously stirred at 160 °C for 24 h. After cooling to room temperature, the solvent was evaporated under reduced pressure. The product was used for the next step without further purification.

3,4-Diphenyl-4H-1,2,4-triazole. 2-Phenyl-1,3,4-oxadiazole (9.0 g, 62 mmol), phenylamine (5.7g, 61.5 mmol), and *o*-dichlorobenzene (30 mL) were combined into a 100 mL round-bottom flask equipped with a stir bar, condenser and N₂ bubbler. Trifluoroacetic acid (4.7 mL, 61.4 mmol) was added, and the reaction mixture was refluxed at 182 °C for 16 h. After cooling to room temperature, it was poured into 10% aqueous sodium carbonate (200 mL). The mixture was adjusted to pH~10 and then transferred to a separatory funnel. The product was extracted with dichloromethane two times. The organic layers were combined and washed with brine, dried over MgSO₄, and concentrated under reduced pressure. *o*-Dichlorobenzene was vacuum distilled at 90 °C to give a white solid (8.1 g, 60%).

3-Bromo-4,5-diphenyl-4H-1,2,4-triazole. A 500 mL round-bottom flask was charged with 3,4-diphenyl-4H-1,2,4-triazole (7.1 g, 32 mmol), *N*-bromosuccinimide (7.2 g, 40.0 mmol), carbon tetrachloride (60 mL), and acetic acid (60 mL). The flask was heated at 120°C. The reaction was monitored by TLC (3:2 CH₂Cl₂: EtOAc) after 4 h to show a product forming. After 4.5 h, more *N*-bromosuccinimide (1.5 g) was added to the reaction. After 6.5 h, TLC showed a faint spot corresponding to the starting triazole. The flask was lifted out after 7.75 h. Aqueous Na₂CO₃ (10%) was added to the

reaction mixture until the pH was ~ 8. The product was extracted with CH₂Cl₂ three times, and the combined organic solution was washed with brine, dried over MgSO₄, filtered, concentrated under reduced pressure to give the faint yellow solid (7.6 g, 80%).

3-(2-Methoxyphenyl)-4,5-diphenyl-4H-1,2,4-triazole. A 500 mL, 2-neck round-bottom flask was charged with 3-bromo-4,5-diphenyl-4H-1,2,4-triazole (9.0 g, 23 mmol), 2-methoxy benzyl boronic acid (7.1 g, 46.8 mmol), toluene (200 mL), and K₃PO₄ monohydrate (16.2 g, 70.3 mmol). In the glovebox, Pd(dba)₃ (0.43 g, 0.47 mmol), S-Phos (0.77 g, 1.9 mmol), and toluene (30 mL) were combined in a sealed round-bottom flask and stirred at room temperature for 20 minutes. The catalyst solution was quickly transferred to the reaction outside of the glovebox. The reaction was heated for 10 h and concentrated. The resulting residue was purified by silica gel column chromatography (eluent EtOAc: Hexanes = 1:1), which gave dark brown powder (2.3 g, 30%).

2-(4,5-Diphenyl-4H-1,2,4-triazol-3-yl)phenol. To a mixture of 3-(2-methoxyphenyl)-4,5-diphenyl-4H-1,2,4-triazole (1.5 g) in 20 mL CH₂Cl₂ at -78 °C was added BBr₃ (1.25 g, 50 mmol in 20 mL CH₂Cl₂) dropwise. The mixture was stirred for 24 h at -78 °C and the resulting solution was poured into water, extracted with CH₂Cl₂ (50 mL × 3 times) and the solvent was removed under and recrystallization of the residue from ethanol gave dark brown solid (**dpdp**). Then, to a suspension of **dpdp** (1.3g) in methanol (30 mL) was added the equivalent KOH in methanol (5 mL) and stirred for 2 hr at room temperature. Concentration in vacuum precipitated a dark brown solid (**Kdpdp**). ¹H NMR (400 MHz, CDCl₃) δ 10.33 (s, 1H), 7.45-7.40 (m, 3H), 7.34-7.31 (m, 2H), 7.27-7.24 (m, 2H), 7.22-7.17 (m, 3H), 6.90 (t, *J* = 7.5 Hz, 2H), 6.75 (d, *J* = 7.5 Hz, 2H). ESI-MS, *m/z*: calcd for C₂₀H₁₅N₃O, 313.12 [M]; found 312.08 [M-H].

General synthesis of Ir(III) complexes. The IrCl₃ (0.64 g, 2.14 mmol) and 2.4 equivalent of cyclometalated ligand (5.14 mmol) were added in a 2-ethoxyethanol and water mixture. Then, the solution was heated for 16 h at 110 °C. After the addition of water, the precipitated yellow powder was filtered and reacted with **Kdpdp** without further purification for another 16 h at 110 °C. After cooling, the solution was concentrated and the resulting residue was purified by silica gel column chromatography (CH₂Cl₂/petroleum ether 1:2 (v/v)) and vacuum sublimation gave yellow-green crystals.

Ir-TN₃T: Yield: 72.0%. ¹H NMR (400 MHz, CDCl₃) δ 9.19 (dd, *J* = 1.12, 5.70 Hz, 1H), 8.49-8.47 (m, 2H), 8.34 (d, *J* = 8.41 Hz, 1H), 7.93 (t, *J* = 8.01 Hz, 1H), 7.77 (t, *J* = 8.00 Hz, 1H), 7.54-7.46 (m, 3H), 7.33 (dd, *J* = 5.17, 12.43 Hz, 3H), 7.19 (dd, *J* = 9.93, 18.02 Hz, 4H), 6.96 (dd, *J* = 6.91, 19.31 Hz, 3H), 6.89 (s, 1H), 6.82 (t, *J* = 8.65 Hz, 1H), 6.55 (s, 1H), 6.38-6.35 (m, 2H), 6.11 (t, *J* = 7.52 Hz, 1H). HR-MS, *m/z*: calcd for C₄₄H₂₄N₇F₁₂OIr, 1087.1480 [M]; found 1088.1560

[M+H]⁺. Anal. Calcd for C₄₄H₂₄N₇F₁₂OIr: C, 48.62; H, 2.23; N, 9.02. Found: C, 48.67; H, 2.32; N, 9.24%.

Ir-TN₄T: Yield: 75.0%. ¹H NMR (400 MHz, CDCl₃) δ 8.99 (d, *J* = 5.62 Hz, 1H), 8.22 (d, *J* = 5.65 Hz, 1H), 8.04-7.99 (m, 4H), 7.76 (t, *J* = 7.81 Hz, 1H), 7.62 (t, *J* = 8.52 Hz, 1H), 7.46 (dt, *J* = 7.21, 24.73 Hz, 4H), 7.31 (t, *J* = 7.50 Hz, 1H), 7.17 (dd, *J* = 6.54, 14.08 Hz, 4H), 6.90-6.88 (m, 2H), 6.75-6.68 (m, 2H), 6.27 (ddd, *J* = 1.20, 3.55, 8.38 Hz, 2H), 6.04 (t, *J* = 7.55 Hz, 1H). HR-MS, *m/z*: calcd for C₄₄H₂₄N₇F₁₂OIr, 1087.1480 [M]; found 1088.1565 [M+H]⁺. Anal. Calcd for C₄₄H₂₄N₇F₁₂OIr: C, 48.62; H, 2.23; N, 9.02. Found: C, 48.74; H, 2.47; N, 9.32%.

Acknowledgements

This work was supported by the National Natural Science Foundation of China (51773088).

Notes and references

¹Jiangsu Key Laboratory of Atmospheric Environment Monitoring and Pollution Control, Collaborative Innovation Center for Atmospheric environment and equipment technology, College of Environmental Science and Engineering, Nanjing University of Information Science & Technology, Nanjing 210044, P. R. China *E-mail: 002083@nuist.edu.cn

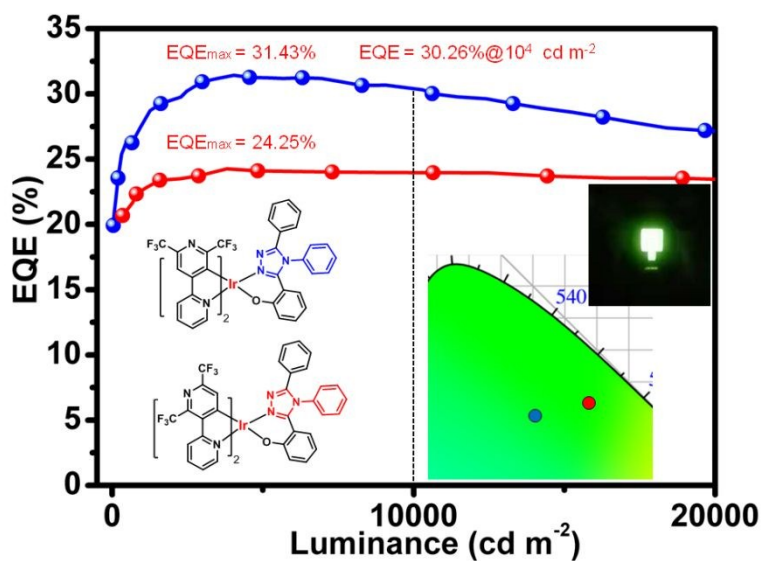
²State Key Laboratory of Coordination Chemistry, Collaborative Innovation Center of Advanced Microstructures, School of Chemistry and Chemical Engineering, Nanjing University, Nanjing 210093, P. R. China, *E-mail: yxzhang@nju.edu.cn

³Shenzhen Key Laboratory of Polymer Science and Technology, College of Materials Science and Engineering, Shenzhen University, Shenzhen 518060, P.R. China, *E-mail: gzhu@szu.edu.cn

†Electronic Supplementary Information (ESI) available: Details of materials and measurements. Synthesis details of the cyclometalated ligand. Details of X-ray Crystallography, electrochemical tests and theoretical calculation. Procedures of OLEDs fabrication and measurements. The crystallographic data of iridium complexes. The electronic cloud density distribution, TG curves, cyclic voltammograms and selected lifetime curves of complexes. Current efficiency versus luminance of device with different doped concentrations.

- (a) S. Lamansky, P. Djurovich, D. Murphy, F. Abdel-Razzaq, H.-E. Lee, C. Adachi, P. E. Burrows, S. R. Forrest and M. E. Thompson, *J. Am. Chem. Soc.*, 2001, **123**, 4304; (b) W.-Y. Wong and C.-L. Ho, *J. Mater. Chem.*, 2009, **19**, 4457; (c) W.-Y. Wong and C.-L. Ho, *Coord. Chem. Rev.*, 2009, **253**, 1709; (d) H. T. Cao, L. Ding, J. Yu, G. G. Shan, T. Wang, H. Z. Sun, Y. Gao, W. F. Xie and Z. M. Su, *Dyes Pigm.*, 2019, **160**, 119.
- (a) L. Li, W.-C. Chow, W.-Y. Wong, C.-H. Chui and R. S.-M. Wong, *J. Organomet. Chem.*, 2011, **696**, 1189; (b) H. Zhan, W.-Y. Wong, A. Ng, A. B. Djuricic and W.-K. Chan, *J. Organomet. Chem.*, 2011, **696**, 4112; (c) J. Zhang, F. C. Zhao, X. J. Zhu, W.-K. Wong, D. G. Mg and W.-Y. Wong, *J. Mater. Chem.*, 2012, **22**, 16448; (d) M. Hissler, W. B.

- Connick, D. K. Geiger, J. E. McGarrah, D. Lipa, R. J. Lachicotte and R. Eisenberg, *Inorg. Chem.*, 2000, **39**, 447; (e) S.-C. Chan, M. C. W. Chan, Y. Wang, C.-M. Che, K.-K. Cheung and N. Zhu, *Chem. Eur. J.*, 2001, **7**, 4180; (f) J. Brooks, Y. Babayan, S. Lamansky, P. I. Djurovich, I. Tsyba, R. Bau and M. E. Thompson, *Inorg. Chem.*, 2002, **41**, 3055; (g) Z. M. Hudson, C. Sun, M. G. Helander, Y. L. Chang, Z. H. Lu and S. Wang, *J. Am. Chem. Soc.*, 2012, **134**, 13930; (h) X. L. Yang, G. J. Zhou and W.-Y. Wong, *Chem. Soc. Rev.*, 2015, **44**, 8484; (i) G. J. Zhou, W.-Y. Wong and X. L. Yang, *Chem. Asian J.*, 2011, **6**, 1706; (j) C.-L. Ho, H. Li and W.-Y. Wong, *J. Organomet. Chem.*, 2014, **751**, 261.
3. (a) M. A. Baldo, D. F. O'Brien, Y. You, A. Shoustikov, S. Sibley, M. E. Thompson and S. R. Forrest, *Nature*, 1998, **395**, 151; (b) R. C. Kwong, S. Lamansky and M. E. Thompson, *Adv. Mater.*, 2000, **12**, 1134; (c) H. Sasabe and J. Kido, *Chem. Mater.*, 2011, **23**, 621; (d) C.-L. Ho and W.-Y. Wong, *New J. Chem.*, 2013, **37**, 1665; (e) X. B. Xu, X. L. Yang, J. Zhao, G. J. Zhou and W.-Y. Wong, *Asian J. Org. Chem.*, 2015, **4**, 394.
4. (a) C. L. Ho, L. C. Chi, W. Y. Hung, W. J. Chen, Y. C. Lin, H. Wu, E. Mondal, G. J. Zhou, K. T. Wong and W. Y. Wong, *J. Mater. Chem.*, 2012, **22**, 215; (b) G. J. Zhou, C. L. Ho, W. Y. Wong, Q. Wang, D. G. Ma, L. X. Wang, Z. Y. Lin, T. B. Marder and A. Beeby, *Adv. Funct. Mater.*, 2008, **18**, 499; (c) L. L. Wen, X. G. Hou, G. G. Shan, W. L. Song, S. R. Zhang, H. Z. Sun and Z. M. Su, *J. Mater. Chem. C*, 2017, **5**, 10847; (d) K. Y. Zhao, H. T. Mao, L. L. Wen, G. G. Shan, Q. Fu, H. Z. Sun and Z. M. Su, *J. Mater. Chem. C*, 2018, **6**, 11686.
5. (a) H. H. Fong, K. C. Lun and S. K. So, *Chem. Phys. Lett.*, 2002, **353**, 15407; (b) S. Heun and P. M. Borsenberger, *Chem. Phys.*, 1995, **200**, 245.
6. (a) H. Movla, *Optic.*, 2015, **126**, 5237; (b) W.-Y. Hung, P.-Y. Chiang, S.-W. Lin, W.-C. Tang, Y.-T. Chen, S.-H. Lin, P.-T. Chou, Y.-T. Hung and K.-T. Wong, *ACS Appl. Mater. & Interfaces*, 2016, **8**, 4811; (c) H. Mu, D. Klotzkin, A. D. Silva, H. P. Wager, D. White and B. Sharpton, *Appl. Phys. Lett.*, 2008, **41**, 235109; (d) C.-L. Ho, W.-Y. Wong, B. Yao, Z. Y. Xie, L. X. Wang and Z. Y. Lin, *J. Organomet. Chem.*, 2009, **694**, 2735; (e) X. L. Yang, Z. Huang, J. S. Dang, C.-L. Ho, G. J. Zhou and W.-Y. Wong, *Chem. Commun.*, 2013, **49**, 4406; (f) G. J. Zhou, X. L. Yang, W.-Y. Wong, Q. Wang, S. Suo, D. G. Ma, J. K. Feng and L. X. Wang, *ChemPhysChem*, 2011, **12**, 2836; (g) G. J. Zhou, Q. Wang, X. Z. Wang, C.-L. Ho, W.-Y. Wong, D. G. Ma, L. X. Wang and Z. Y. Lin, *J. Mater. Chem.*, 2010, **20**, 7472; (h) G.-J. Zhou, W.-Y. Wong, B. Yao, Z. Y. Xie and L. X. Wang, *J. Mater. Chem.*, 2008, **18**, 1799.
7. (a) Y. C. Zhu, L. Zhou, H. Y. Li, Q. L. Xu, M. Y. Teng, Y. X. Zheng, J. L. Zuo, H. J. Zhang and X. Z. You, *Adv. Mater.*, 2011, **23**, 4041; (b) H. Y. Li, L. Zhou, M. Y. Teng, Q. L. Xu, C. Lin, Y. X. Zheng, J. L. Zuo, H. J. Zhang and X. Z. You, *J. Mater. Chem. C*, 2013, **1**, 560; (c) Q. L. Xu, C. C. Wang, T. Y. Li, M. Y. Teng, S. Zhang, Y. M. Jing, X. Yang, W. N. Li, C. Lin, Y. X. Zheng, J. L. Zuo, X. Z. You, *Inorg. Chem.*, 2013, **52**, 4916.
8. (a) J. A. Kitchen, J. Olguin, R. Kulmaczewski, N. G. White, V. A. Milway, G. N. L. Jameson, J. L. Tallon and S. Brooker, *Inorg. Chem.*, 2013, **52**, 11185; (b) R. W. Hogue, H. L. C. Feltham, R. G. Miller and S. Brooker, *Inorg. Chem.*, 2016, **55**, 4152; (c) S. I. Vasylevs'kyy, G. A. Senchyk, A. B. Lysenko, E. B. Rusanov, A. N. Chernega, J. Jezierska, H. Krautscheid, K. V. Domasevitch and A. Ozarowski, *Inorg. Chem.*, 2014, **53**, 3642.
9. (a) Q. Wang, J. Ding, D. Ma, Y. Cheng, L. Wang, X. Jing and F. Wang, *Adv. Funct. Mater.*, 2009, **19**, 84; (b) F.-M. Hsu, C.-H. Chien, P.-I. Shih and C.-H. Cheng, *Chem. Mater.*, 2009, **21**, 1017; (c) J. H. Kim, D. Y. Yoon, J. W. Kim and J.-J. Kim, *Synth. Met.*, 2007, **157**, 743.
10. (a) P. Tao, W. L. Li, J. Zhang, S. Guo, Q. Zhao, H. Wang, B. Wei, S. J. Liu, X. H. Zhou, Q. Yu, B. S. Xu and W. Huang, *Adv. Funct. Mater.*, 2016, **26**, 881; (b) C. H. Lin, J. L. Liao, Y. S. Wu, K. Y. Liao, Y. Chi, C. L. Chen, G. H. Lee and P. T. Chou, *Dalton Trans.*, 2015, **44**, 8406; (c) J. B. Kim, S. H. Han, K. Yang, S. K. Kwon, J. J. Kim and Y. H. Kim, *Chem. Commun.*, 2015, **51**, 58; (d) S. H. Lee, S. O. Kim, H. Shin, H. J. Yun, K. Yang, S. K. Kwon, J. J. Kim and Y. H. Kim, *J. Am. Chem. Soc.*, 2013, **135**, 14321.
11. Y. T. Tao, C. L. Yang and J. G. Qin, *Chem. Soc. Rev.*, 2011, **40**, 2943.
12. (a) Q. L. Xu, X. Liang, S. Zhang, Y. M. Jing, X. Liu, G. Z. Lu, Y. X. Zheng and J. L. Zuo, *J. Mater. Chem. C*, 2015, **3**, 3694; (b) F. Jerald, D. V. Giang, D. M. Charles, C. G. Troy, P. Kyung-Ho, S. M. Jeffrey, J. M. Will, B. Joseph, M. B. Lois, D. D. Kerwin, H. S. Thomas and G. Z. Steve, *Organometallics*, 2015, **34**, 3665.
13. (a) L. Ying, C.-L. Ho, H. B. Wu, Y. Cao and W.-Y. Wong, *Adv. Mater.*, 2014, **26**, 2459; (b) X. L. Yang, G. J. Zhou and W.-Y. Wong, *J. Mater. Chem. C*, 2014, **2**, 1760; (c) X. B. Xu, X. L. Yang, J. S. Dang, G. J. Zhou, Y. Wu, H. Li and W.-Y. Wong, *Chem. Commun.*, 2014, **50**, 2473; (d) X. B. Xu, X. L. Yang, Y. Wu, G. J. Zhou, C. Wu and W.-Y. Wong, *Chem. Asian J.*, 2015, **10**, 252.
14. (a) A. P. Wilde and R. J. Watts, *J. Phys. Chem.*, 1991, **95**, 622; (b) M. G. Colombo, T. C. Brunold, T. Riedener, H. U. Gudel, M. Fortsch and H. B. Burgi, *Inorg. Chem.*, 1994, **33**, 545.
15. (a) S.-Y. Kim, W.-I. Jeong, C. Mayr, Y.-S. Park, K.-H. Kim, J.-H. Lee, C.-K. Moon, W. Brütting and J.-J. Kim, *Adv. Funct. Mater.*, 2013, **23**, 3896; (b) K. Udagawa, H. Sasabe, C. Cai and J. Kido, *Adv. Mater.*, 2014, **26**, 5062; (c) J.-H. Lee, S.-H. Cheng, S.-J. Yoo, H. Shin, J.-H. Chang, C.-I. Wu, K.-T. Wong and J.-J. Kim, *Adv. Funct. Mater.*, 2015, **25**, 361; (d) C.-Y. Lu, M. Jiao, W.-K. Lee, C.-Y. Chen, W.-L. Tsai, C.-Y. Lin and C.-C. Wu, *Adv. Funct. Mater.*, 2016, **26**, 3250.
16. I. D. Parker, *J. Appl. Phys.*, 1994, **75**, 1656.



Two novel iridium(III) complexes containing the electron-transporting group of 4-phenyl-4*H*-1,2,4-triazole showed good photoluminescence and electroluminescence performances with EQE of 31.43% and mild efficiency roll-off.